ROBERT J. KARREN*
U. S. Geological Survey
Washington, D.C. 20242

Camera Calibration by the Multicollimator Method

An evaluation shows that the values of radial lens distortion have an error of only two microns.

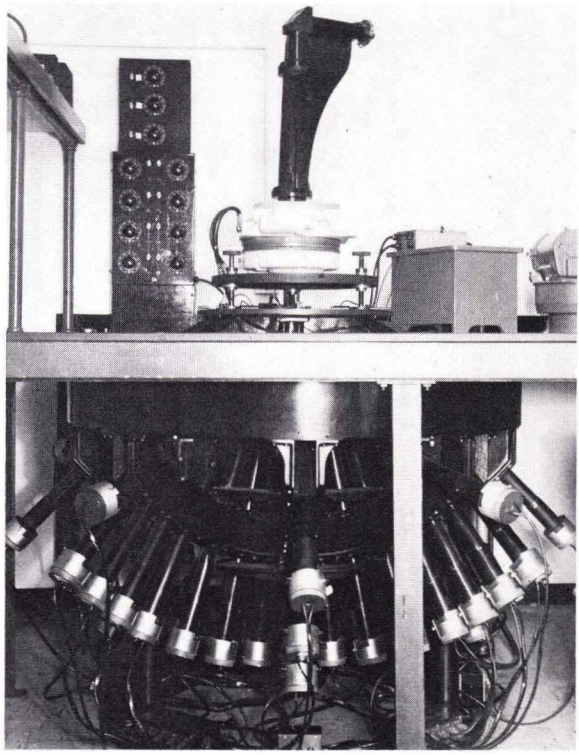

FIG. 1. The U. S. Geological Survey multicollimator.

INTRODUCTION

SINCE 1953, THE U. S. Geological Survey has used a multicollimator (Figure 1) for checking the cameras used to provide photographs for photogrammetric compilation of topographic maps. In particular, the calibrator has been used to determine whether the cameras used by contractors are capable of furnishing aerial photographs that can be used satisfactorily in the Survey's photogrammetric equipment.

With the advent of analytical aerotriangulation methods, however, the calibrator was called on to assume a new and additional function—that of providing precise data on lens distortion for use in refining image coordinate data for input to the computations. Accordingly, an evaluation of the multicollimator calibration system was undertaken to determine the accuracy of the lens distortion values that it yields.

For this evaluation, a series of glass-plate negatives was exposed in a Wild RC8 aerial camera on the multicollimator and measured on a Mann monocular comparator. The angular positions of the collimators were measured, computational procedures were adapted or developed to obtain the required parameter values, and error analyses were made whenever possible to determine the probable accuracy of the parameter values.

SOURCES OF ERROR

MEASUREMENT OF COLLIMATOR ANGLES

A special theodolite assembly is used to determine the angular positions of the collimators. This assembly is shown in Figure 2. The lower part is a modified Wild T2 theodolite from which the horizontal circle has been removed and a reversed T3 vertical bearing installed to compensate for the downward thrust. This instrument was further modified by Wild so that the perpendicularity

* Presented at the Semi-Annual Convention of the American Society of Photogrammetry, St. Louis, Mo., 1967 under the title "An Evaluation of Aerial Camera Calibration by the Multicollimator Method." Publication authorized by the Director, U. S. Geological Survey.

of the two axes can be accurately set each time the instrument is used to measure radial angles. The upper instrument is a standard T2 theodolite which is used to measure horizontal angles. To compensate for unsymmetric weight distribution, it was necessary to add weights A and B as shown in the photograph.

Each angle, horizontal and vertical, was measured four times—two times with the theodolite telescope erect and two times with the telescope plunged, with one direct and one reverse angle forming a set. The standard errors for the horizontal angle were:

Standard error of a single set ±3.17 seconds
Standard error of the mean ±2.24 seconds.

Similar values for the vertical angles were:

Standard error of a single set ±0.99 second
Standard error of the mean ±0.70 second.

It should be noted that the standard error values given above are an indication of the precision of repeating the measurements and do not represent absolute accuracy, as one or more systematic errors may be involved. As a comparison, Washer (1956) gives a value of ±2 seconds as the probable error of measuring a vertical angle on the multicollimator at the National Bureau of Standards.

ABSTRACT: *An evaluation of the multicollimator method of aerial camera calibration used by the U. S. Geological Survey yields a standard error in radial distortion of two microns. The study was undertaken partly because of the special needs of analytic aerotriangulation and includes statistical analyses of the residual errors of focal length, point of symmetry, tilt of the focal plane, radial and tangential lens distortions. The study is based on the collineation principle as a mathematical model, employing the solution of the resection problem, and applying least squares.*

MEASUREMENT OF IMAGE COORDINATES

The images of the collimator targets as they appear in the field of a wide-angle camera are shown in Figure 3. The coordinates of each target were measured four times, and each measurement was corrected to a standard temperature. The standard error for each set of measurements was computed. The *average* standard error of a single measurement was obtained by averaging the standard errors for all sets, with the following results:

$$m_x = m_y = \pm 1.4 \text{ microns.}$$

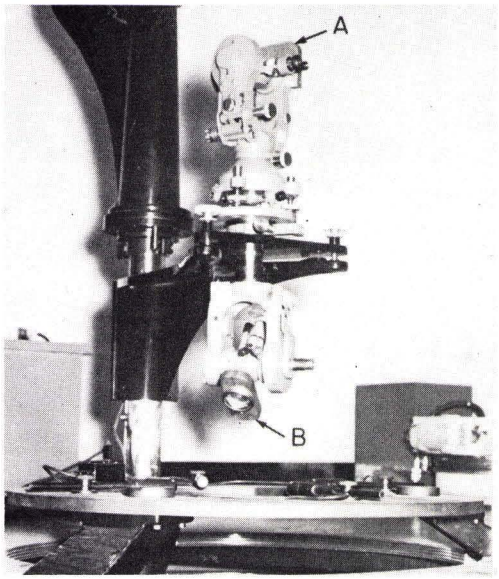

FIG. 2. Special Wild theodolite assembly for measuring collimator angles.

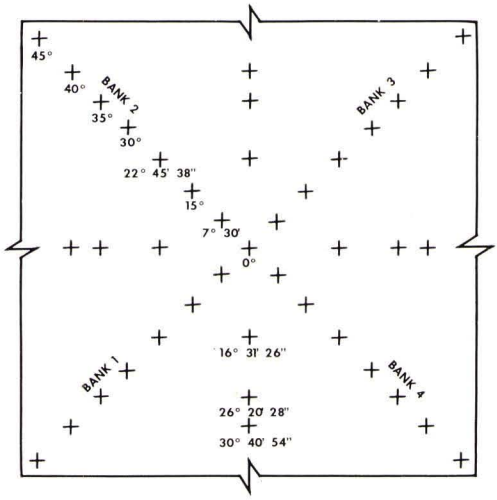

FIG. 3. Target images recorded by a wide-angle camera.

GLASS-PLATE CURVATURE

The departure of a glass plate from a plane surface can introduce a significant amount of error into the computer collimator positions because the photographic exposure is a central perspective, whereas the measurements are made orthogonally to the surface of the plate. The amount of distortion can be expressed as

$$D = S \tan \beta = S\, r/f,$$

where

β = angle of incidence of image ray
S = deviation from flatness
r = radial distance from camera axis
f = focal length.

Table 1 shows the distortion introduced at various angles of incidence when the deviation from flatness is 5 and 10 microns.

Usually a glass plate will not exhibit a uniform curvature but will have a varying curvature or waviness. Nevertheless, significant departures from flatness may be encountered unless special attention is paid to this plate characteristic.

The glass plates now used to make the multicollimator exposures have a flatness tolerance of 0.00002 inch per linear inch. The metric equivalent of this tolerance is 0.2 microns per linear centimeter. Thus, even though the tolerance may be additive over a portion of the plate, the errors due to lack of flatness will not be significant.

EMULSION DISTORTION

Errors in plate coordinates can be caused by distortion of the photographic emulsion. This distortion may be local or platewide in extent, and can be caused by photographic processing, temperature and humidity changes, etc. For example, Brucklacher and Luder (1956) reported nonuniform dimensional errors of ± 2.4 microns after measuring the intersections on a glass plate which had been exposed to a grid. The emulsion distortion on a glass-plate negative is usually very small.

TABLE 1. EFFECT OF PLATE CURVATURE
($f = 152.70$ mm)

Radial Angle	*Distortion (D) in Microns*	
	S = 5 microns	*S = 10 microns*
7.5°	0.6	1.3
15.0	1.3	2.6
22.5	2.1	4.2
30.0	2.9	5.8
35.0	3.5	7.0
40.0	4.2	8.4
45.0	5.0	10.0

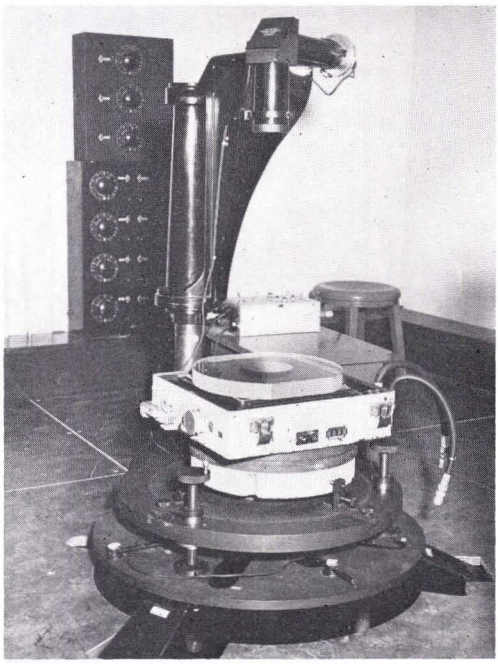

FIG. 4. Plane-parallel plate used for positioning aerial camera on multicollimator.

TILT OF IMAGE PLANE

When positioning the aerial camera on the multicollimator for calibration, the camera lens axis should be made to coincide with the axis of the central collimator, and the focal plane should be normal to this axis. To attain these conditions, a thick optical plane-parallel plate which has a mirrored top surface is placed on the focal plane of the camera as shown in Figure 4. The position of the camera is adjusted with the leveling screws until the images in the auto-collimator coincide. The focal plane of the camera should then be normal to the central collimator axis. In practice, this condition is often not quite achieved, leaving a small tilt of the focal plane which results in a displacement of the collimator target images. This displacement will cause errors in the values of lens distortion.

DETERMINATION OF CALIBRATION PARAMETERS

THEORETICAL CONSIDERATIONS

If we are to make reliable photogrammetric measurements, then there should be an

exact correspondence between the light rays entering the camera and the light rays that leave the lens and produce images on the focal plane. The purpose of camera calibration is to determine the deviation of the image bundle from the object bundle so that corrections may be applied to the image bundle.

In order to compare the image and object bundles, it is necessary to make some assumptions. The primary assumption is that a photograph is a perspective representation. This assumption provides that all rays entering the pupil of the camera lens meet at a single point called the exterior perspective center. This perspective center is necessary if we are to define the object angles. A second assumption is that the objects are at an infinite distance from the camera and that the light rays from these objects are straight lines. This assumption is valid when photographing multicollimator targets because the collimators throw parallel beams of light similar to those from an infinite distance, and there is no atmospheric refraction to bend the light rays.

Two sets of values can be determined for camera calibration: (1) the object angles between the center collimator and the other collimators, and (2) the distances between the collimator target images on the image plane. In order to relate the object angles and image distances, it is necessary to assume the existence of a second point called the interior perspective center. This point is the origin of angles to the image points, and the distance of this point from the image plane is the focal length or camera constant. The principal point is the foot of the perpendicular from the interior perspective center to the image plane.

It should be emphasized that the exterior and interior perspective centers are fictitious points which cannot be located physically within the lens system. In actuality, the aerial camera lens system is highly complex and cannot be compared optically with a perspective projection.

Also, it should be emphasized that the distortion is not necessarily uniform around the lens axis. It can be best described as a vector quantity with a given magnitude and direction. This vector can be resolved into radial and tangential components. In addition, the lens axis is not usually a straight line but follows a variable path because the lens elements are not centered perfectly. This is described as the bent-axis effect. This effect tends to make the distortion unsymmetrical around the point of autocollimation. Lens decentering also influences the magnitude and direction of the distortion vector. Again, this is an oversimplification of the actual lens characteristics, but it serves to define the two effects in which we are most interested: (1) the magnitude and direction of distortion, and (2) the asymmetry of distortion.

We encounter problems when we try to define a point of origin for coordinate values on the image plane. The principal point was defined as the foot of the perpendicular from the interior perspective center. The interior perspective center is defined, in turn, as the point at which the perspective rays to the plate images enclose the same angles as the perspective object rays enclose at the exterior perspective center, in a perfect camera. Because there are very few perfect cameras in existence, the interior perspective center is undefined for our purposes. If we had a perfect camera, the point of autocollimation, the point of symmetry, and the principal point would coincide. Because they do not, we must, of necessity, use the point of autocollimation as the origin of our plate measurements and determine, in some manner, the magnitude of the bent-axis effect which has displaced the point of autocollimation away from the principal point

Numerous methods have been proposed to solve this problem. Dr. Washer (1957), of the National Bureau of Standards, uses a principal point that is defined by assuming that the observed departures from axisymmetry are the same as if a thin prism were placed in front of a perfect lens. This prism effect shifts the point of autocollimation away from the principal point. The magnitude of the prism effect and the shift of the principal point are determined from the asymmetry of the distortion around the point of autocollimation. Other methods have been proposed by Roelofs (1951), Mayer (1956), Thompson (1957), and Hallert (1962).

If we remember that our primary purpose is to reconstruct the object bundle of rays, it is apparent that most of the problems mentioned can be resolved by a least-squares solution. If we fit the image bundle to the object bundle (as shown in Figure 5) by the method of least squares, we can locate the interior perspective center, the point of symmetry, and the principal point. We can also determine the calibrated focal length and the tilt of the image plane with respect to the object plane. The solution will provide a direct comparison of the object and image bundles and minimize distortion and the effect of asymmetrical distortion over the whole plate.

Because we are dealing with one plate, the least-squares solution becomes a space-resection problem. This approach has been used by Roelofs (1951) and Hallert (1955). However, neither one uses a full least-squares solution. Roelofs uses a semigraphical solution, and Hallert adjusts only one concentric ring of images at a time and, as a consequence, makes several least-square adjustments to cover a plate.

METHOD OF ADJUSTMENT

There are numerous solutions of the space-resection problem described in the literature—for example, Rapp (1966). The solution by Harris, Tewinkel, and Whitten (1962) was chosen because it offers several advantages. The primary advantage is that the residuals are expressed in terms of the plate coordinates, and it is a simple problem to transform these residuals into distortion values. The mathematics of this solution are fully described in the reference and also appear in the *Manual of Photogrammetry*, 3d ed., published by the American Society of Photogrammetry.

The basic equations for the resection problem in the method used here, are:

$$\begin{aligned}
&x_i[(X_i-X_c)\sin\phi+(Y_i-Y_c)(-\sin\omega\cos\phi)\\
&\quad+(Z_i-Z_c)\cos\omega\cos\phi]\\
&-z[(X_i-X_c)\cos\phi\cos\kappa\\
&\quad+(Y_i-Y_c)(\cos\omega\sin\kappa+\sin\omega\sin\phi\cos\kappa)\\
&\quad+(Z_i-Z_c)(\sin\omega\sin\kappa-\cos\omega\sin\phi\cos\kappa)]=0 \qquad (1)\\
&y_i[(X_i-X_c)\sin\phi+(Y_i-Y_c)(-\sin\omega\cos\phi)\\
&\quad+(Z_i-Z_c)\cos\omega\cos\phi]\\
&-z[(X_i-X_c)(-\cos\phi\sin\kappa)\\
&\quad+(Y_i-Y_c)(\cos\omega\cos\kappa-\sin\omega\sin\phi\sin\kappa)\\
&\quad+(Z_i-Z_c)(\sin\omega\cos\kappa+\cos\omega\sin\phi\sin\kappa)=0
\end{aligned}$$

where X_i, Y_i, Z_i are object coordinates, X_c, Y_c, Z_c are coordinates of the camera station, and x_i, y_i, z are image coordinates. These equations express the collinearity of three points in space—an object, its image, and the lens point. The image coordinates are measured from the plates made on the multicollimator. The object coordinates are the coordinates of the collimator targets. We know the radial angles to the collimators at the exterior perspective center. We also know the horizontal angles between collimators which were measured around the axis of the center collimator. We can convert these angular values into a fixed coordinate system by passing an imaginary plane through the object bundle perpendicular to the axis of the center collimator and at a suitable distance from the point of convergence of the object rays. The intersection of this plane and the object rays provide horizontal positions for the collimator targets. This situation is illustrated in Figure 5.

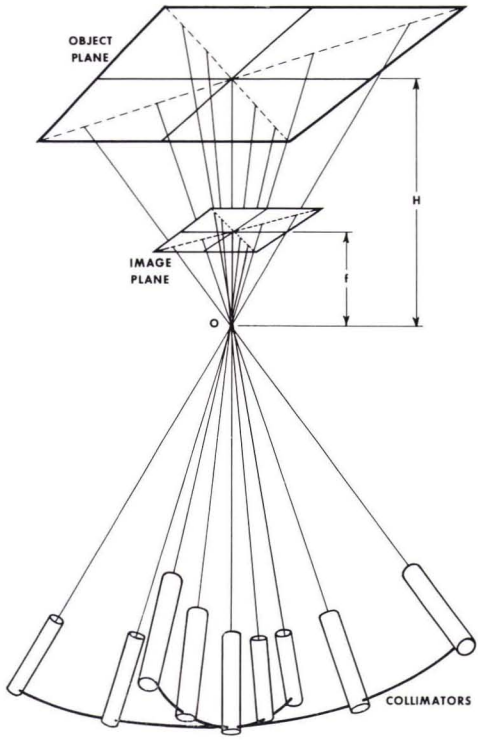

FIG. 5. The resection solution adapted for use with multicollimator data.

The lens point, in this case, is the point of convergence of the collimator axes, which is also the exterior perspective center. Since we are fitting the image bundle to the object bundle, the interior and exterior perspective centers will coincide. The distance from this combined perspective center (point O in figure 5) to the object plane is arbitrarily chosen to be

$$H_c = 10f \qquad (2)$$

where f is the assumed focal length. The coordinates of the collimator targets in the object plane are

$$\begin{aligned}
X_i &= H_c\tan\beta_i\cos(\alpha_i+45)\\
Y_i &= H_c\tan\beta_i\sin(\alpha_i+45)\\
Z_i &= \text{constant} = 0
\end{aligned} \qquad (3)$$

where β_i is the radial angle of the i-th collimator and α_i is the aximuth of the i-th collimator in the object plane. The azimuths are measured clockwise from the collimator at a radial angle of 45 degrees in collimator bank 1

(see Figure 3). The angular value of 45 degrees is added so that the origin of the azimuths coincides with the X-axis.

Solution of the resection problem will give us the coordinates of the perspective center X_c, Y_c, H_c in terms of the object coordinate system and the rotational values ω, ϕ, κ for the image plane. We start with approximate values of the unknowns and solve for corrections dX_c, dY_c, dH_c, $d\omega$, $d\phi$, $d\kappa$ to these approximate values. The origin of the object coordinates is the point where the axis of the center collimator intersects the object plane. Since we made the object plane perpendicular to the center collimator axis, the X and Y coordinates of the perspective center will also be zero. Therefore, the approximate values of the perspective center coordinates may be taken as 0, 0, H_c where H_c is defined in Equation 2. The approximate values of ω, ϕ, and κ may be set equal to zero because their values will be small.

In this adjustment, the object coordinates, the image coordinates, and the focal length are fixed quantities and do not change. The coordinates of the perspective center and rotational elements of the image plane are allowed to change until a *best fit* is obtained between the bundle of object rays and the bundle of image rays. In this manner, the image residuals (including distortion) will be minimized. We do not obtain the principal point and calibrated focal length directly, because only the perspective center coordinates are allowed to change. However, if we make the object and image planes coincide, we can obtain these values.

Originally, we made the distance from the perspective center to the object plane H_c greater than the distance to the image plane f by a factor of 10. If we reduce the value of H_c obtained from the adjustment by the same factor, we will obtain the position where the image plane should be. This position will differ from the actual position of the image plane by the amount of change between the assumed focal length and the calibrated focal length. The reason for this difference is that we held the shape of the cone of image rays fixed and allowed the shape of the object cone of rays to change. Therefore, if we correct the assumed focal length by an amount equal to and opposite in sign from the change in H_c (divided by 10), we obtain the calibrated focal length. If we divide the X and Y coordinates of the perspective center by 10, we obtain the coordinates of the point of symmetry in the image plane. This point will be the principal point (as previously defined) only if the image plane is parallel to the object plane. This will be the case when the tilt values (ω and ϕ) are equal to zero. Otherwise, the location of the principal point can be calculated, if needed, from the values of tilt and focal length.

Analyses of Results

Error Determination

The values of the coordinates of the point of symmetry, the calibrated focal length, and the ω and ϕ tilts of the image plane are obtained directly or indirectly from values of the unknowns which were computed in the resection adjustment. There are two methods by which we can obtain the precision of these values. The first method compares the adjusted values from each set of plate measurements. The second method obtains the standard errors from the individual adjustments. To do this, we compute the inverse of the normal equations, or the inverse weight matrix. The inverse weight matrix is multiplied by the variance factor and the result is the variance-covariance matrix from which we can compute the standard errors of the unknowns in the adjustment. The variance factor (or variance of unit weight) is obtained from the expression

$$m_0^2 = \frac{[vv]}{2n - 6} \tag{4}$$

where $[vv]$ is the sum of the squares of the image residuals and n is the number of observations or, in this case, the number of collimator target images measured.

The image residual is the distance on the image plane between the image point and the intersection of the image plane with the line between the perspective center and the object point after adjustment. The image residuals are composed of lens distortion, image measurement error, collimator angle measurement error, and errors from other sources. We wish to find the magnitude of the lens distortion and we wish to know the effect of the other errors on the determination of distortion and the unknowns in the adjustment. In other words, we want an image residual that does not include lens distortion. There is no way to separate these errors within the adjustment, and the desired image residual must be obtained in some other way.

The desired image residual can be found by combining the plate and angular measurement errors. This determination, however, will not contain the errors from other sources, such as plate curvature. An alternative method is to determine the image residuals

TABLE 2. RESULTS FROM ADJUSTMENT OF POINTS OF EQUAL RADIUS

Plate No.	*Radius mm.*	*Focal Length mm.*	*Principal X mm.*	*Point Y mm.*	*ω Min.*	*φ Min.*	*κ Min.*	m_0 *mm.*	m_f *mm.*
1	20	152.331	−0.093	−0.024	0.55	−2.07	8.03	±0.0020	±0.0077
	41	152.312	−0.038	−0.025	−0.50	−0.81	8.15	0.0030	0.0056
	64	152.294	−0.018	0.001	0.01	−0.35	8.15	0.0036	0.0031
	88	152.281	−0.007	−0.005	0.12	−0.16	8.07	0.0027	0.0024
	106	152.274	−0.010	−0.004	0.10	−0.18	8.14	0.0029	0.9021
	128	152.276	−0.006	0.002	−0.01	−0.08	8.11	0.0034	0.0020
3	20	152.346	0.042	−0.033	0.74	0.97	16.82	0.0018	±0.0070
	41	152.321	−0.012	0.000	0.00	−0.27	16.89	0.0020	0.0037
	64	152.303	0.006	0.005	−0.10	0.16	16.86	0.0025	0.0030
	88	152.288	0.000	0.000	−0.02	−0.01	16.91	0.0020	0.0017
	106	152.279	−0.003	−0.006	0.10	−0.04	16.92	0.0033	0.0024
	128	152.278	0.000	−0.004	0.06	0.01	16.90	0.0035	0.0021
5	20	152.352	0.024	−0.025	0.54	0.54	8.03	0.0009	±0.0030
	41	152.331	0.016	−0.028	0.58	0.36	7.98	0.0019	0.0030
	64	152.309	0.008	−0.019	0.37	0.16	8.02	0.0017	0.0020
	88	152.292	0.006	−0.005	0.07	0.15	7.99	0.0031	0.0030
	106	152.284	0.006	−0.006	0.08	0.14	8.10	0.0022	0.0010
	128	152.280	0.004	−0.010	0.14	0.11	8.08	0.0028	0.0030

Note: m_0 = Standard error of unit weight.
m_f = Standard error of focal length.

from a separate adjustment using the center collimator image and images of equal radius, as in the method of Hallert (1962). Because the lens distortion is mostly radial, the adjustment will remove the effect of distortion by changing the focal length. The residuals will then be composed mostly of measurement and other errors, along with some asymmetric and tangential lens distortion. This method should give us a fair approximation of the variance factor while excluding most lens distortion.

Six separate adjustments were made on each of three plates and the results are listed in Table 2. An average value for the variance factor of the image residuals was computed from this table and used for the adjustments using all of the points on a plate.

TABLE 3. CALIBRATED FOCAL LENGTHS

Odd-numbered Plates		*Even-numbered Plates*	
Plate No.	*Focal Length*	*Plate No.*	*Focal Length*
1	152.280 mm	2	152.299 mm
1*R*	152.282	2R	152.291
3	152.285	4	152.296
3*R*	152.279	4R	152.291
5	152.289	6	152.297
7	152.283	8	152.294
Mean	152.283	Mean	152.294
m_f	±0.0036	m_f	±0.0026

Note: *R* indicates a repeat measurement on a plate.

CALIBRATED FOCAL LENGTH

The value of the calibrated focal length as determined by the resection adjustment will minimize radial distortion over the area of the plate covered by the calibration. Values for the calibrated focal length are given in Table 3. The odd-numbered plates contain more image points, and image points at greater distances from the principal point. Consequently the calibrated focal length from these plates will not agree with the calibrated focal length from the even-numbered plates. For this reason, the values are listed separately in Table 3.

LOCATION OF POINT OF SYMMETRY

The coordinates of the point of symmetry obtained from the space resection adjustment are listed in Table 4 along with the coordinates of the point of autocollimation. Both sets of coordinates have fiducial mark 1 as their origin.

The standard errors of the coordinates of the point of symmetry are quite large, as shown in Table 4. Here, the standard errors for the point of symmetry are larger than those for the point of autocollimation. Variations in tilt between the various plates will

TABLE 4. COORDINATES OF THE POINT OF SYMMETRY

Plate No.	*Point of Autocollimation*		*Point of Symmetry*	
	X	*Y*	*X*	*Y*
1	105.986 mm.	105.997 mm.	105.978 mm.	105.999 mm.
1*R*	105.981	105.996	105.978	105.998
2	105.992	105.997	105.992	106.002
2*R*	105.982	105.999	105.981	106.001
3	105.998	105.996	105.994	105.994
3*R*	105.985	105.997	105.985	105.990
4	105.999	105.995	105.998	105.995
4*R*	105.980	105.995	105.986	105.999
5	105.991	105.992	105.997	105.986
6	105.980	105.995	105.971	105.983
7	105.980	105.997	105.972	105.995
8	105.979	105.997	105.965	105.997
Mean Values				
All Plates	105.986	105.996	105.983	105.995
m	±0.007	±0.002	±0.011	±0.006
Plates 1–8	105.988	105.996	105.983	105.994
m	±0.008	±0.002	±0.013	±0.006
Plates 1*R*–4*R*	105.982	105.997	105.983	105.997
m	±0.002	±0.002	±0.004	±0.005

cause variations in the location of the point of symmetry.

From the variance-covariance matrix obtained from the computer program, we find the correlation between the perspective center coordinates and the tilt elements. The coefficient of correlation between X and ϕ is

$$r_{x\phi} = \frac{m_{x\phi}}{(m_x^2 + m_\phi^2)^{\frac{1}{2}}} = 0.981. \qquad (5)$$

Furthermore,

$$m_y^2 = m_x^2$$

and

$$m_\omega^2 = m\phi^2$$

$$r_{y\omega} = r_{x\phi} = 0.981$$

where m_x^2, m_ϕ^2, m_y^2, and m_ω^2 are variances and $m_{x\phi}$ and $m_{y\omega}$ are covariances. The value of r indicates a very high degree of correlation between X and ϕ and Y and ω. This condition implies that any tilt of the image plane will be reflected in the coordinates of the perspective center. The effect on the point of symmetry will be the same, because its coordinates are obtained directly from those of the perspective center. Consequently, precise leveling of the focal plane during autocollimation and flatness of the glass-plate negative are essential for accurate location of the point of symmetry.

The standard errors of the adjusted values of the perspective center coordinates (as given by the adjustment of one plate) are

$$m_x = m_y = \pm 2.7 \text{ microns.}$$

If we consider the correlation between the coordinates of the perspective center and the ω and ϕ tilts, the standard errors of the adjusted values of the coordinates will be

$$m_x = \pm (m_x^2 + f^2 m_\phi^2 + 2f m_{x\phi})^{\frac{1}{2}} = \pm 3.0 \text{ microns}$$
$$m_y = \pm (m_y^2 + f^2 m_\omega^2 - 2f m_{y\omega})^{\frac{1}{2}} = \pm 3.0 \text{ microns} \qquad (6)$$

where m_x^2, m_ω^2, m_y^2, and m_ϕ^2 are variances and $m_{x\phi}$, $m_{y\omega}$ are covariances. The standard errors for the coordinates of the point of symmetry will be the same.

Carmen (1961) states that the error of principal-point location is ±10 microns at a confidence limit of 99 percent* for results obtained from the multicollimator at the Applied Physics Division of the National Research Council of Canada. He does not state the number of plates that were measured. In our case, the 99.7 percent confidence limit for the adjusted values for a single plate is ±9 microns. For the determination from the average of 12 sets of plate measurements, the error at the 99.7 percent confidence limit is ±31.8 microns for the X-coordinate and ±16.8 microns for the Y-coordinate. Similar

* It is assumed that this is a confidence limit of 99.7 percent, which is equal to three times the standard error.

values for the standard error of the mean are ±9 microns and ±6 microns.

ROTATIONAL ELEMENTS

The values of ω, ϕ, and κ are listed in Table 5. The tilt values (ω and ϕ) show a considerable variation, and a pattern is not discernible. They are small; the maximum tilt is 15 seconds of arc, and the mean is very small. The standard error of the adjusted values is

$$m_\omega = m_\phi = \pm 0.053 \text{ minutes}$$

for the odd-numbered plates, and

$$m_\omega = m_\phi = \pm 0.080 \text{ minutes}$$

for the even-numbered plates. The mean values are smaller than the standard errors and, for practical purposes, there is no tilt of the image plane. This means the point of symmetry very nearly coincides with the principal point, in this case. The variation in the tilt values and the variation in the location of the point of symmetry are related, and both are caused by measurement error, plate curvature, and lack of precision in the autocollimating procedure. The value of κ depends on the alignment of the camera over the banks of collimators and has very little significance since the exact location of the collimator images is not critical. They should be near the diagonals or axes of the plate.

RADIAL LENS DISTORTION

Radial distortion values were computed from twelve sets of plate measurements. The odd-numbered plates provided values along the plate diagonals, and the even-numbered plates provided values along the plate axes. Figure 6 shows the designation and location of the collimator targets.

The values of the radial distortion along the diagonals and the mean values for each diagonal are listed in Table 6. The largest standard error is ±2.4 microns, and the standard errors are consistent over the plate. The relatively large errors for the point-of-symmetry determination apparently are not reflected in the radial distortion values.

TABLE 5. ROTATIONAL ELEMENTS

Plate No.	*ω minutes*	*φ minutes*	*κ minutes*
1	0.00	−0.13	8.12
1*R*	−0.04	−0.04	8.06
2	−0.12	0.01	8.80
3*R*	−0.05	0.03	8.78
3	0.03	−0.05	16.90
3*R*	0.11	0.02	16.90
4	−0.03	−0.01	24.31
4*R*	−0.15	0.23	24.37
5	0.11	0.14	8.06
6	0.25	−0.11	−8.05
7	0.03	−0.08	6.41
8	0.03	−0.02	19.84
Mean	0.014	−0.018	11.875

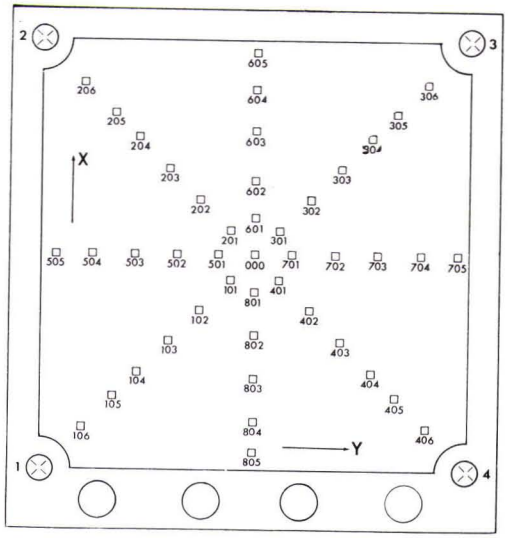

FIG. 6. Location and designation of collimator targets.

The distortion curves for the mean radial distortion along each diagonal are shown in Figure 7. Figure 8 shows the mean distortion curve obtained by averaging the distortion values from four diagonals. This curve is identical to the curve obtained by meaning the unadjusted radial distortion values and changing the focal length from the assumed value of 152.270 mm to the adjusted value of 152.283 mm. This change is obtained by use of the expression

$$\Delta D = \Delta f \tan \beta \qquad (7)$$

where ΔD is the change in radial distortion resulting from Δf, which is the change in focal length.

The values of radial distortion along the diagonals before adjustment are tabulated in Table 7, and the distortion curves are shown in Figure 9. The standard errors are smaller after adjustment.

Table 8 lists the adjusted values of radial distortion along the plate axes. The distortion curves along each axis are shown in Figure 10, and the mean distortion curve is shown in Figure 11. The standard errors are similar in magnitude to the standard errors for radial distortion along the diagonals.

The calibrated focal length obtained from the adjustment of the even-numbered plates

TABLE 6. RADIAL DISTORTION ALONG THE PLATE DIAGONALS

Target No.	Plate Number 1	1R	3	3R	5	7	Mean	m_D
101	6	7	7	10	10	7	7.8	±1.7
102	8	9	9	10	11	10	9.5	1.0
103	4	6	4	4	9	6	5.5	2.0
104	0	2	1	1	−1	1	0.7	1.0
105	−5	−7	− 6	−7	−4	−10	−6.5	2.4
106	−8	−8	−10	−9	−9	−10	−9.0	0.9
201	7	7	11	12	10	8	9.2	2.1
202	9	9	11	12	14	11	11.0	1.9
203	7	8	11	9	11	10	9.3	1.6
204	2	5	2	2	5	5	3.5	1.6
205	−2	−2	− 1	0	−4	0	−1.5	1.5
206	0	−4	− 2	−4	−7	− 2	−3.2	2.1
301	4	8	6	5	7	4	5.7	1.5
302	5	9	8	8	10	9	8.2	1.7
303	6	8	6	4	5	5	5.7	1.4
304	−4	−4	− 1	1	−1	− 1	−1.7	2.0
305	−7	−6	− 8	−7	−4	− 9	−6.8	1.7
306	−5	−7	− 9	−9	−7	− 9	−7.7	1.6
401	10	9	8	10	7	10	9.0	1.2
402	12	12	10	13	10	10	11.2	1.3
403	9	7	9	6	8	10	8.3	1.2
404	4	3	5	5	4	2	3.8	1.2
405	−2	−3	− 1	0	−3	− 1	−1.7	1.2
406	−2	−2	− 3	−5	−6	0	−3.0	1.7

Mean Radial Distortion

Radius	Distortion
20 mm.	7.9
41	10.0
64	7.2
88	1.6
106	−4.1
128	−5.7

Note: All distortion values are in microns.

is not the same as the value obtained from the odd-numbered plates because the number of images and the area of the plate considered were not the same. In order to make the axial radial distortion compatible with the diagonal radial distortion, the focal length is changed and the distortion recomputed according to Equation 7. The mean distortion curves before and after the focal length change are shown in Figure 11. The mean distortion curve for the plate diagonals is also shown. An inspection of Figure 11 shows that the agree-

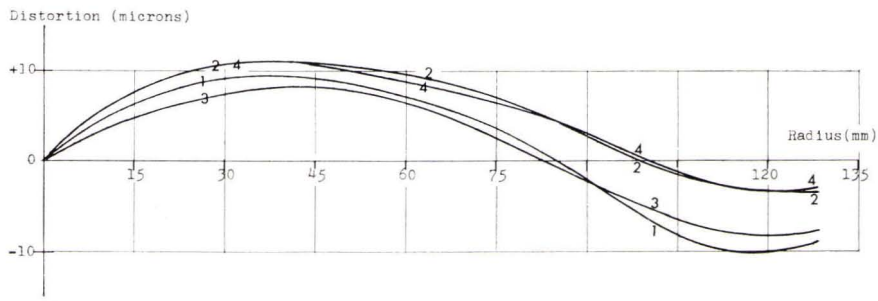

FIG. 7. Mean radial distortion along the plate diagonals.

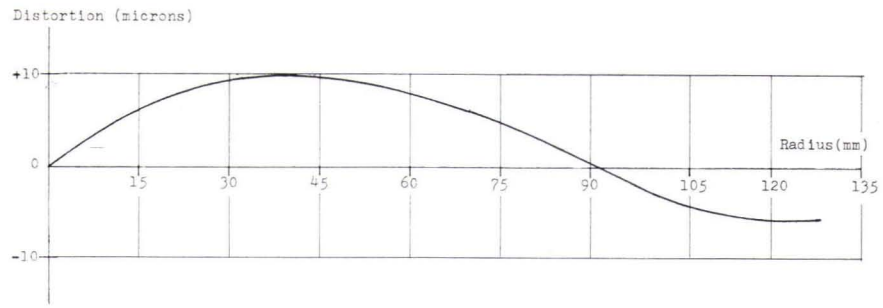

FIG. 8. Mean radial distortion obtained by averaging the radial distortion along the diagonals.

TABLE 7. RADIAL DISTORTION ALONG THE PLATE DIAGONALS BEFORE ADJUSTMENT

Target No.	*Plate Number*						*Mean*[a]	*Mean*[b]	m_D
	1	*1R*	*3*	*3R*	*5*	*7*			
101	8	8	7	9	10	6	8.0	6.3	±1.3
102	11	11	11	11	14	10	11.3	7.8	1.3
103	9	10	10	6	15	9	9.8	4.4	2.8
104	7	8	8	5	8	5	6.8	−0.7	1.4
105	3	−1	4	0	6	−2	2.4	−6.7	3.3
106	3	0	2	−1	4	0	1.5	−9.4	2.1
201	10	9	12	12	10	14	11.4	9.7	1.8
202	14	13	15	13	18	18	15.0	11.5	2.1
203	12	13	17	13	18	18	15.2	9.8	2.8
204	10	11	11	8	15	15	11.8	4.3	2.8
205	6	7	10	8	12	12	9.0	−0.1	2.5
206	8	5	10	5	12	11	8.6	−2.3	3.0
301	5	10	9	8	11	8	8.6	6.9	2.0
302	7	13	14	12	16	14	12.8	9.3	3.1
303	7	13	13	8	15	12	11.4	6.0	3.1
304	2	4	8	7	12	8	6.8	−0.7	3.6
305	−2	3	4	1	11	2	3.2	−5.9	4.3
306	0	3	4	−1	11	3	3.3	−7.6	4.3
401	9	10	10	13	11	8	10.1	8.4	1.9
402	12	13	13	15	16	10	13.4	9.9	2.3
403	11	11	15	11	16	12	12.7	7.3	2.4
404	8	9	13	10	14	7	10.2	2.7	2.9
405	5	5	8	5	8	5	6.0	−3.1	1.5
406	8	8	9	1	6	8	6.4	−4.5	2.9

Note: All distortion values are in microns.
[a] Mean of distortion values along diagonals for focal length of 152.270 mm.
[b] Mean of distortion values along diagonals for focal length of 152.283 mm.

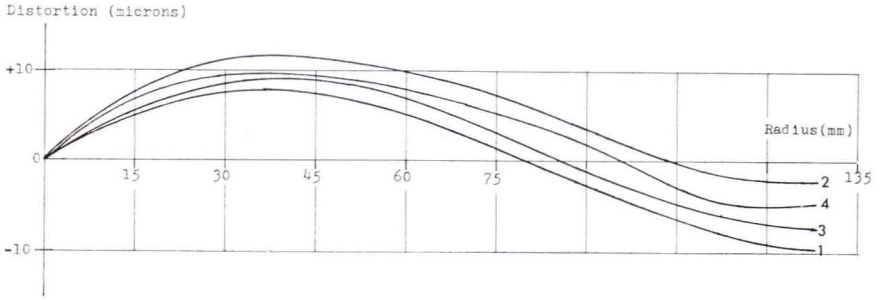

FIG. 9. Mean radial distortion along the plate diagonals before adjustment.

TABLE 8. RADIAL DISTORTION ALONG THE PLATE AXES

Target No.	*2*	*2R*	*4*	*4R*	*6*	*8*	*Mean*	*m*
501	7	10	7	10	7	7	8.0	±1.5
502	10	12	8	11	13	9	10.5	1.9
503	6	9	7	6	9	6	7.2	1.5
504	2	4	−1	1	−1	1	1.0	1.9
505	− 8	− 7	−7	− 4	−10	− 8	−7.3	1.9
601	8	8	7	6	7	8	7.3	0.8
602	8	8	10	10	8	8	8.7	1.0
603	7	6	7	5	7	5	6.2	1.0
604	− 2	− 6	−1	− 3	1	− 1	− 2.0	2.4
605	− 9	−11	−9	−12	− 9	− 8	− 9.7	1.5
701	7	9	8	7	5	7	7.2	1.3
702	11	11	9	8	7	6	8.7	2.1
703	7	10	5	9	5	5	6.8	2.2
704	0	2	0	2	0	− 2	0.3	1.5
705	− 8	− 6	−7	− 5	− 9	− 5	− 6.7	1.6
801	7	4	5	9	10	8	7.2	2.3
802	9	8	8	7	8	10	8.3	1.0
803	5	4	5	5	8	6	5.5	1.4
804	− 1	− 2	0	− 1	0	0	− 0.7	1.8
805	−10	−12	−9	−12	− 8	−10	−10.0	1.7

Mean Radial Distortion

Radius	*Distortion*
20 mm.	7.4
41	9.0
64	6.4
88	−0.4
106	−8.4

Note: All distortion values are in microns.

ment between the axial and diagonal values is poor. The maximum separation is about 5 microns.

The same separation exists between the mean distortion curves before adjustment. In this case, the focal length used for both determinations was 152.270 mm. Therefore, the adjustment can be eliminated as a cause of the separation. The shape of the two curves is very nearly the same, and an arbitrary change of 5 microns in the focal length would make them coincide.

ACCURACY OF RADIAL DISTORTION VALUES

Three sets of standard errors for radial distortion have been determined from (1) the combination of standard errors of measurement, (2) separate adjustment of images of equal radius, and (3) the average of the adjusted distortion values. A comparison of the standard errors from each source is shown in Table 9.

The values of the standard errors from the three sources agree quite well. The average of all the standard errors listed in Table 9 is

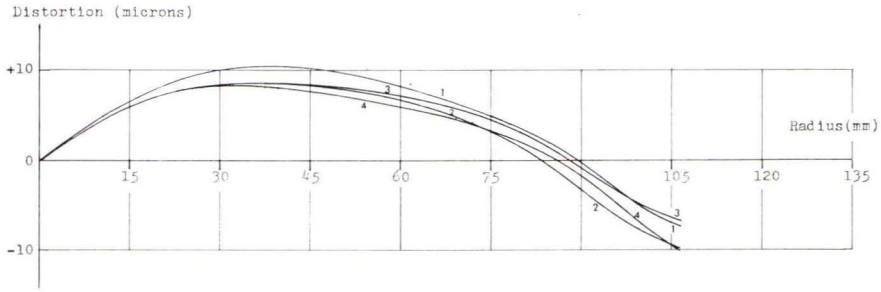

FIG. 10. Radial distortion curves for measurements made along plate axes.

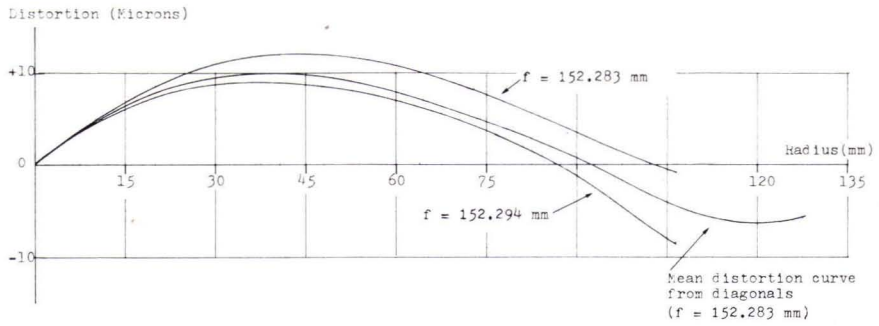

FIG. 11. Comparison of mean distortion curves from diagonal and axial measurements.

± 2.0 microns. If we use a 95.5 percent confidence limit, we can expect that the distortion values from one plate measurement will be accurate within ± 4 microns for 95.5 percent of the images measured. This is true only if our errors follow a normal probability distribution and we have no residual systematic error. Carmen (1961) gives a value of ± 3 microns for the determination of radial distortion with the multicollimator in Canada.

The mean distortion curve determined by Wild Heerbrugg Limited, manufacturer of the camera, is shown in Figure 12. The full curve cannot be compared because the 45-degree collimators of the multicollimator are not visible. However, we can compare the first part of the curves if the distortion for both curves is made to equal zero at the same radial distance, i.e., if both curves cross the abscissa at the same point. If this is done, we find that there is a maximum difference in distortion values of 4 microns and a difference in the calibrated focal length of 9 microns. The time lapse between the two calibrations is over two years.

TANGENTIAL LENS DISTORTION

The effect of tangential distortion makes a straight line passing through the lens axis in object space appear as a curved line on the photograph. The magnitude of tangential distortion is given along a perpendicular to the straight line passing through the principal point and the true position of the image point.

TABLE 9. COMPARISON OF STANDARD ERRORS OF RADIAL DISTORTION

Radius	*(1)**	*(2)**	*(3)**	*Mean*
20 mm.	$\pm 1.6\mu$	$\pm 1.6\mu$	$\pm 1.6\mu$	$\pm 1.6\mu$
41	1.7	2.3	1.5	1.8
64	1.7	2.4	1.6	1.9
88	1.8	2.6	1.6	2.0
106	1.9	2.7	1.7	2.1
128	2.0	3.3	1.6	2.3

* See text for explanation.

The tangential distortion can be obtained from the plate residuals given in the resection adjustment. When the banks of collimators are aligned with the photographic axes, the tangential distortion will be the y-residual along the X-axis and the x-residual along the Y-axis.

If the image points are along the plate diagonals, it is necessary to rotate the residual vectors 45 degrees so that they will fall on and perpendicular to the diagonal.

As with radial distortion, the accuracy of tangential distortion will depend on the accuracy of the measurements of the collimator angles and image coordinates. The standard errors of measuring these values are listed again here:

$$m_x = \pm 1.4 \text{ microns}$$
$$m_y = \pm 1.4 \text{ microns}$$
$$m_\beta = \pm 1.0 \text{ seconds}$$
$$m_\alpha = \pm 3.2 \text{ seconds}.$$

If we set $\beta = 30°$ and $\alpha = 45°$, and combine these measurement errors according to the law of error propagation, the standard error of tangential distortion as determined from one plate measurement will be ± 3.4 microns. Consequently, unless the tangential distortion is larger than about 4 microns, we cannot say that it is tangential distortion and not measuring error.

CONCLUSIONS

The computational methods used in this paper provide values for all of the parameters of aerial camera calibration. The use of a least-squares solution gives values based on all of the measurements instead of just certain portions. Values have been obtained by a direct comparison of the image and object

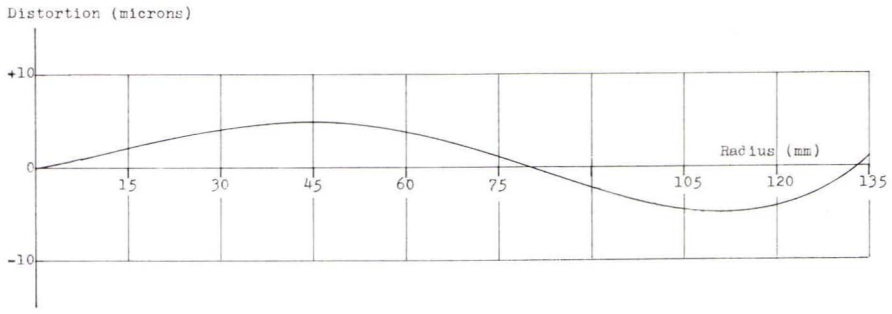

FIG. 12. Mean distortion curve from Wild Heerbrugg Ltd.

bundles, thus facilitating reconstruction of the object bundle. In addition, standard errors are computed to aid in evaluating the consistency and accuracy of the results.

The error analyses have provided estimates of the accuracy of the values for the various parameters. However, it must be remembered that the estimates made from a statistical error analysis are valid only for accidental errors that follow the normal distribution pattern. Various errors of a systematic nature may exist that have not been accounted for. Such systematic errors degrade the validity of the estimates unless they can be isolated and removed.

Keeping in mind the preceding limitations, estimates of the accuracies of the various parameters are summarized in Table 10. These estimates are based on a 95.5 percent confidence limit and are listed for the calibration results from a single plate and for the combined results from four plates. For parameters which have coordinate values, the value listed in Table 10 is for both coordinates. If there was a significant difference between the error values for the coordinates, the higher value was used.

There is reason to believe that the results of analytical aerotriangulation could be improved if lens distortion could be determined at a greater number of positions more uniformly distributed across the photograph. This however, is a subject for another study. The research at hand, however, shows that the values of radial lens distortion at the collimator positions are surprisingly accurate. In fact, the value of ± 2 microns is approaching the measuring accuracy of most comparators.

TABLE 10. ACCURACY ESTIMATES FOR CALIBRATION VALUES

Parameters	*Estimates*	
	1 Plate	*4 Plates*
Fiducial Coordinates	$\pm$ 4μ	$\pm$ 2μ
Indicated Principal Point	4	2
Fiducial Distances	4	2
Point of Autocollimation	14	7
Point of Symmetry	21	11
Calibrated Focal Length	8	4
Radial Distortion	4	2
Tangential Distortion	7	4

REFERENCES

Brucklacher, W. A., and Luder, W., "Untersuchung über die Schrümpfung von Messfilmen und photographischen Plattenmaterial," Deutsche Geodätische Kommission bei der Bayerischen Akademie der Wissenschaften, Munchen, *Applied Geodesy*, Series B, *31*.

Carmen, P. D., and Brown, H., 1961, "Camera Calibration in Canada," *Canadian Surveyor*, vol. 15, no. 8, p. 425–439.

Hallert, B., 1955, "A New Method for the Determination of the Distortion and the Inner Orientation of Cameras and Projectors," *Photogrammetria*, vol. 11, no. 3, p. 107–115.

Hallert, B., 1962, "Investigations of Basic Geometric Quality of Aerial Photographs," *GIMRADA Research Note* No. 4, DDC Document No. AD297351

Harris, W. D., Tewinkel, G. C., and Whitten, C. A., 1962, Analytic Aerotriangulation, U. S. Coast and Geodetic Survey *Technical Bulletin* No. 21.

Mayer, I., 1956, "The Presentation of the Results of Camera Calibration," *Photogrammetria*, vol. 11, no. 2, p. 49–66.

Rapp, R. H., 1966, "Comparison of Space Resection Adjustments," *Journal of the Surveying and Mapping Division*, ASCE, no. SU1.

Roelofs, R., 1951, "Distortion, Principal Point, Point of Symmetry, and Calibrated Principal Point," *Photogrammetria*, vol. 7, no. 2, p. 49–66.

Thompson, E. H., 1957, "The Geometrical Theory of the Camera and its Application to Photogrammetry," *The Photogrammetric Record*, vol. 2, no. 10, p. 241–262.

Washer, F. E., 1956, "Sources of Error in Various Methods of Airplane Camera Calibration," PHOTOGRAMMETRIC ENGINEERING, vol. 22, no. 4, p. 722–740.

Washer, F. E., 1957, "The Effect of Prism on the Location of the Principal Point," PHOTOGRAMMETRIC ENGINEERING, vol. 23, no. 3 p. 520–532.